Received January 25, 2021, accepted February 10, 2021, date of publication February 22, 2021, date of current version March 3, 2021.

Digital Object Identifier 10.1109/ACCESS.2021.3061134

Optimal Design of Joint Protomatrix for DP-LDPC Codes-Based JSCC System Over on-Body Channel

DAN SONG [1], LIN WANG [1] (Senior Member, IEEE), QIWANG CHEN [2], AND GUANRONG CHEN [3], (Life Fellow, IEEE)

[1]Department of Information and Communication Engineering, Xiamen University, Xiamen 361005, China
[2]Xiamen Key Laboratory of Mobile Multimedia Communications, Huaqiao University, Xiamen 361021, China
[3]Department of Electrical Engineering, City University of Hong Kong, Hong Kong

Corresponding author: Lin Wang (wanglin@xmu.edu.cn)

This work was supported in part by the National Natural Science Foundation of China under Grant 61671395 and Grant 61871337, in part by the Science Foundation of Fujian Province, China, under Grant 2020J05056, and in part by the Scientific Research Funds of Huaqiao University under Grant 20BS105.

ABSTRACT A high-quality data transmission scheme in wireless body area networks is implemented by a joint source-channel coding (JSCC) system with M-ary differential chaos shift keying modulation over an on-body channel. Current DP-LDPC code pairs, which have shown good bit-error ratio performance over additive white Gaussian noise channel and Rayleigh fading channel, cannot perform well over on-body channel. In this paper, the DP-LDPC codes are redesigned for the JSCC system with new methods depending on the on-body channel characteristics. A protomatrix dimension-restrictive searching algorithm for DP-LDPC codes in the JSCC system is proposed according to the on-body channel bandwith and source statistic, which is effective to predesign the dimension of the code pair for a new JSCC system. In this way, the source-channel code rates are appropriately allocated to leave more source redundancy for improving the error floor. Moreover, the joint protomatrix is reconstructed into two kinds of compact structures by simplifying the edge linking relationships and modifying joint protograph extrinsic information transfer algorithm, which decreases the induction of searching entries to further accelerate the code searching speed. The searched code pairs show better bit-error ratio performances compared with existing DP-LDPC codes. The power consumption in the new joint coding system is lower than the separate coding system in WBAN on the physical layer.

INDEX TERMS Joint source-channel coding, DP-LDPC codes, on-body channel, M-ary DCSK modulation, bit-error ratio.

I. INTRODUCTION

Wireless body area networks (WBAN) are breakthrough technologies implemented in medical services via equipping lightweight devices onto human body. These equipments collect data by monitoring physical conditions to detect chronic diseases [1]. According to the IEEE 802.15 report [2], log-normal distribution is chosen as an on-body channel model because it matches well in most cases as is shown in Table 1.

TABLE 1. Summary of the best fitting distributions for on-body channel in case of still postures.

Position	Distribution	Position	Distribution
Right wrist	Normal	Right upper arm	Log-normal
Head	Weibull	Right ear	Normal
Shoulder	Log-normal	Chest	Log-normal
Right rib	Log-normal	Left waist	Normal
Right thigh	Log-normal	Right ankle	Log-normal

To minimize data distortion, the data transmission in WBAN is optimized on the physical layer to achieve a good bit error ration (BER) performance [3]. In this setting, some good error correcting codes are introduced to fulfill the task requirements, including the protograph low-density parity check (P-LDPC) code [4], [5]. Notice also that the lightweight equipments in WBAN are too small to store power for data transmission [6]. Thus, a low power consumption communication link needs to be designed with a new structure on the physical layer.

The associate editor coordinating the review of this manuscript and approving it for publication was Yi Fang.

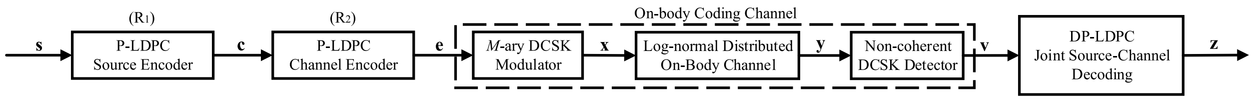

FIGURE 1. Framework of the JSCC system over on-body coding channel with M-ary DCSK modulation.

Therefore, high reliability and low power consumption are two objectives of data transmissions in WBAN [7]. Joint source-channel coding (JSCC) is an integrated model with joint encoding or decoding for high reliability and low power consumption [8]. To well match a new non-standard channel model, the encoder and the decoder need to be redesigned in the separate coding system [29]. Therefore, the coding part in a JSCC system also needs to be modified for the on-body channel model. A code index modulated M-ary differential chaos shift keying (DCSK) system is proposed in [9], which is promising for simultaneously providing energy and transmitting information of the user equipment without any external power supply in eHealthcare. Moreover, the wide frequency band (900MHz, 2.4, 3.1-10.6GHz) [2] of the on-body channel in WBAN is more suitable to be modulated by the M-ary DCSK scheme [10], [12], [13]. In fact, there are two channel models to construct the transmission link in WBAN by the M-ary DCSK scheme. One is the ultra wide band channel model, and the other is to select the channel model from the IEEE 802.15 standard. In this paper, the multipath channel is not considered due to the spectral spreading signal and we use the statistical models of the path loss communication because there are not path loss models for spectral spreading communication in WBAN. Thus, a higher quality data transmission over on-body channel (IEEE 802.15 standard) in WBAN can be obtained with M-ary DCSK-modulated JSCC system. The framework of this JSCC system is shown in Figure 1.

The utilization of the double protograph low-density parity-check (DP-LDPC) codes in the JSCC system can minimize the distortion in medical imaging over additive white Gaussian noise (AWGN) channel [15]. Furthermore, it has been observed that the existing DP-LDPC codes, which have shown good BER performance over AWGN channel [16], [18]–[20] and Rayleigh fading channel (RFC) [11], [17], cannot well perform over non-standard channels. The DP-LDPC code pairs designed in [11] present grave error floors in such an on-body channel system. Considering the compatibility and the sensibility of a JSCC system, to overcome the error floor disadvantage, the source-channel code pairs are redesigned in this paper with new methods to match the characteristics of the on-body channel.

The dimensions of the DP-LDPC code pairs should be firstly determined in a JSCC system and the decoding performance depends on the optimal code rate of the P-LDPC code. More source redundancy is introduced by properly allocating the code rates to improve the channel decoding performance in the JSCC system [14]. Furthermore, the source-channel code rates are defined by the dimensions of the protomatrices of the DP-LDPC codes which are predesigned under bound limitation, i.e., the protomatrix dimension-restrictive searching (PDRS) algorithm. When the optimal dimensions of the protomatrices are determined, the objective DP-LDPC codes with fixed code rates are searched by the differential evolution (DE) algorithm [18], [20]. Generally, the PDRS algorithm is designed with universality for different DP-LDPC code pairs over different channel models.

The DP-LDPC code pairs are generally considered as a joint protomatrix with edge linking relationship in tanner graph [11], [21], [22]. In this way, more indices of entries of two linking matrices in joint protomatrix are introduced into the DE algorithm with high searching complexity. The joint protomatrix used in [11] is simplified to be two kinds of compact structures with less indices of linking entries in the objective joint protomatrix, which is an efficient way to accelerate the DE searching speed. It should be noted that the joint protograph extrinsic information transfer (JPEXIT) algorithm needs to be modified simultaneously by decreasing the entries for better decoding performance.

Here, three contributions in designing a JSCC system are presented: (1) A data transmission of on-body channel in WBAN is optimally designed by the JSCC system based on the DP-LDPC codes on the physical layer, which has better waterfall regions than that in [11] and lower power consumptions than that in [3]. (2) The source-channel code pair is predesigned by the PDRS algorithm limited with the source-channel code rate bound according to the on-body channel bandwith and source statistic. (3) The joint protomatrix is reconstructed to be two kinds of simpler structures according to the new edge linking relationships in the JPEXIT algorithm to decrease the searching indices of entries.

II. SYSTEM MODEL

A. ENCODER BASED ON DP-LDPC CODES

A sparse binary sequence $\mathbf{s}$ is generated by a binary symmetric i.i.d nonuniform memoryless source with probability p, which is the probability of sending "1" satisfying $0 < p < 0.5$. $\mathbf{s}$ is compressed by a source code at rate R_1 and is protected by a channel code at rate R_2. The source-channel codes are expressed by protomatrices of order $c_\imath \times \nu_\jmath$, where c and ν are the numbers of check nodes (CNs) and variable nodes (VNs) respectively, and $\imath$ and $\jmath$ are nodes.

Now, consider a check matrix $\mathbf{H}_{sc}$ of the source code, the source coding sequence is

$$\mathbf{c} = \mathbf{H}_{sc}\mathbf{s}. \tag{1}$$

Then, $\mathbf{c}$ is protected by a transposed calculated generator matrix $\mathbf{G}_{cc}^{T}$ of the channel code as a transmitting sequence,

$$\mathbf{e} = \mathbf{G}_{cc}^{T}\mathbf{c}. \tag{2}$$

The entropy of the source is:

$$H(p) = -p\log_2 p - (1-p)\log_2(1-p). \tag{3}$$

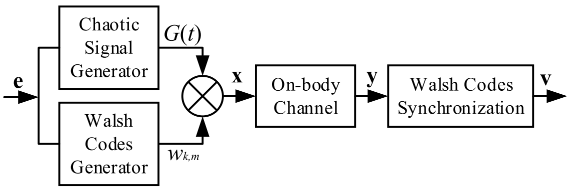

FIGURE 2. The *M*-ary DCSK modulation over the on-body channel.

B. M-ARY DCSK MODULATOR AND DEMODULATOR

The encoded symbols $\mathbf{e}$ is modulated by an original chaotic sequence in Figure 2. The chip interval of each chaotic sample is $T_c = 1$, the smallest time unit. The encoded sequence $\mathbf{e}$ of length n is modulated into a symbol sequence, $\mathbf{x} = \{X_1, \ldots, X_m, \ldots, X_M\}$, $m \in \{1, \ldots, M\}$, by Gray mapping, and the corresponding M-ary symbol is obtained with a vector of the Walsh code matrix. Then, the modulated X_m is generated by

$$X_m = \Sigma_{i=0}^{\varsigma-1} \Sigma_{k=1}^{M} \omega_{k,m} G(t-i), \tag{4}$$

where $\omega_{k,m}$ is the kth element in the mth column of the Walsh code matrix of size $M \times M$, $G(t-i)$ is the delay copy of the chaotic sequence $G(t)$, and t is the discrete time variable with the time unit $T_c = 1$. The length of the original generating sequence G_0 is $\varsigma T_c = \varsigma$, where ς is the spreading factor.

Subsequently, $\mathbf{y} = \{Y_1, \ldots, Y_m, \ldots, Y_M\}$ is received as

$$Y_m = h(t) \cdot X_m + n(t), \tag{5}$$

where $n(t) \sim \mathbf{N}(0, \sigma_n^2)$ is Gaussian noise, $h(t) = \alpha\delta(t-\tau)$ is the channel impulse response, α is a single path fading constant coefficient of the on-body channel, and τ is the time delay, which is set shorter than the chaotic signal duration $0 < \tau \leq \varsigma T_c$.

The received $\mathbf{y}$ is demodulated into sequence $\mathbf{v} = \{V_1, \ldots, V_m, \ldots, V_M\}$. The discrete signal is mapped into the same unit as the modulator, and the mth symbol is received as the $\hat{m}$th one. Since the longest transmission delay is shorter than the chaotic spreading factor ($0 \leq \tau \leq \varsigma T_c$), the inter-symbol interference can be neglected [10]. By multiplication with the Walsh code vector, the observed value $V_{\hat{m}}$ is expressed by the energy correlators as

$$V_{\hat{m}} = \Sigma_{i=1}^{\varsigma} \Sigma_{k=1}^{M} [\alpha\omega_{k,m} G(i-\tau) Q + n_k(i)\omega_{k,\hat{m}}]^2, \tag{6}$$

where $Q = \Sigma_{k=1}^{M} \omega_{k,m}\omega_{k,\hat{m}}$ when $m = \hat{m}$, and $n_k(\cdot)$ is Gaussian noise of the kth element.

C. ON-BODY CODING CHANNEL MODEL

The on-body channel is modeled as a log-normal distributed fading channel. The probability density function (PDF) of the modulated random variable X is [2]

$$p(X) = \frac{\lambda}{\sqrt{2\pi}\sigma_n X} \exp\left[-\frac{(10\log_{10}(X) - \mu_n)^2}{2\sigma_n^2}\right], \tag{7}$$

where $\lambda = \frac{10}{\log 10}$ is a constant. The modulated X_m in dB is exchanged into $X = 10^{-\frac{X_m}{10}}$ (value). σ_n and μ_n are the variance and the mean of the Gaussian random variable, respectively, which are related by [23]

$$\mu_n = -\frac{\sigma_n^2}{\lambda} = -\frac{\sigma_n^2}{10/\log 10}. \tag{8}$$

The variance of an on-body coding channel is

$$\sigma_x^2 = \Sigma_{k=1}^{M} (X_k - \mu_n)^2 \cdot p_k, \tag{9}$$

where p_k is the probability of reception of the kth symbol and $\Sigma_{k=1}^{M} p_k = 1$. Assume that all M symbols are equiprobably acquired with

$$\begin{aligned}
\sigma_x^2 &= \Sigma_{k=1}^{M} (X_k - \mu_n)^2 \cdot \Sigma_{k=1}^{M} p_k \qquad (10)\\
&= \Sigma_{k=1}^{M} \left[X_k + \left(\frac{\sigma_n^2}{\lambda}\right)\right]^2\\
&\geq \Sigma_{k=1}^{M} \left[X_k^2 + \left(\frac{\sigma_n^2}{\lambda}\right)^2\right]\\
&\geq \Sigma_{k=1}^{M} \left[\left(\frac{1}{\lambda}\right)^2 X_k^2 + \left(\frac{1}{\lambda}\right)^2 (\sigma_n^2)^2\right] \qquad (11)\\
&\geq \left(\frac{1}{\lambda}\right)^2 \Sigma_{k=1}^{M} (X_k - \sigma_n^2)^2 \qquad (12)\\
&= \left(\frac{1}{\lambda}\right)^2 \Sigma_{k=1}^{M} (X_k - \mu_r)^2. \qquad (13)
\end{aligned}$$

The last Equation (13) is due to the mean of single path RFC $\mu_r = -\lambda\mu_n$. The variance of single path RFC is

$$\sigma_r^2 = \Sigma_{k=1}^{M} (X_k - \mu_r)^2 \cdot p_k. \tag{14}$$

From (10) to (14), the two variances of the on-body coding channel and single path RFC are related:

$$\sigma_x^2 = \left(\frac{1}{\lambda}\right)^2 \sigma_r^2. \tag{15}$$

Here, the log-normal distributed on-body coding channel is modeled as a single path RFC with a specific coefficient $(\frac{1}{\lambda})^2$ for the modified JPEXIT algorithm.

D. SOFT INFORMATION CALCULATION FOR JOINT SOURCE-CHANNEL DECODING

The symbol sequence $\mathbf{v}$ is received through an on-body coding channel via M-ary DCSK modulation. All-zero codeword is also assumed to be transmitted. The log-likelihood ratio (LLR) of the source decoding is

$$\mathcal{L}_{sc} = \log \frac{1-p}{p}. \tag{16}$$

The LLR of the output of the on-body channel is

$$\mathcal{L}_{ch} = \log \frac{p(Y|X=-1)}{p(Y|X=+1)} = \frac{10\log_{10}(Y^2)}{\sigma_n^2}, \tag{17}$$

where $p(Y|X)$ is the channel conditional PDF evaluated at the output Y (Y_m) given the input X.

With the conditional PDF $p(\mathbf{v}|m)$ of the mth received signal vector $\mathbf{v}$ when $m = \hat{m}$ [10], one obtains

$$p(\mathbf{v}|m) = \frac{1}{2Q\sigma_n^2}\left(\frac{V_m}{\alpha^2 Q}\right)^{\frac{\varsigma-2}{4}} \exp\left(-\frac{\alpha^2 Q + V_m}{2Q\sigma_n^2}\right) \times \mathscr{B}_{\frac{\varsigma}{2}-1}\left(\frac{\sqrt{V_m \alpha^2 Q}}{Q\sigma_n^2}\right), \quad (18)$$

where $\alpha^2 = (\frac{1}{\lambda})^2$ is the fading factor of the on-body coding channel, $\mathscr{B}_{\frac{\varsigma}{2}-1}(\cdot)$ represents the $(\frac{\varsigma}{2}-1)$th order modified Bessel function of the first kind, and V_m is the mth soft decision variable defined by $V_{\hat{m}}$ in Eq. (6).

The LLR of the output through the demodulator is

$$\mathcal{L}_{V,out} = \log\left[\frac{\sum_{m\in M_0^k} p(\mathbf{v}|m)p(m)}{\sum_{\hat{m}\in M_1^k} p(\mathbf{v}|\hat{m})p(\hat{m})}\right] = \log\left[\frac{\sum_{m\in M_0^k} V_m^{-\frac{\varsigma-4}{2}} \mathscr{B}_{\frac{\varsigma}{2}-1}\left(\frac{\sqrt{\alpha^2 V_m}}{\sqrt{Q}\sigma_n^2}\right)p(m)}{\sum_{\hat{m}\in M_1^k} V_{\hat{m}}^{-\frac{\varsigma-4}{2}} \mathscr{B}_{\frac{\varsigma}{2}-1}\left(\frac{\sqrt{\alpha^2 V_{\hat{m}}}}{\sqrt{Q}\sigma_n^2}\right)p(\hat{m})}\right], \quad (19)$$

where M_x^k is the kth modulated symbol, which can be retrieved by Gray demapping, $x \in [0, 1]$, $p(m)$ and $p(\hat{m})$ are the prior probability of the symbols m and $\hat{m}$, respectively.

Note that the prior LLR and the extrinsic LLR are exchanged in joint source-channel decoding over many iterations, which are the prior mutual information (PMI) and the extrinsic mutual information (EMI) transmissions between VNs and CNs, respectively. The iteration number is the updating times of PMI and EMI between the source-channel decoders. With increasing iterations, the prior LLR is less correlated with $\mathcal{L}_{ch}$, and the extrinsic LLR tends to a Gaussian-like distribution [24].

III. OPTIMAL DESIGN METHOD FOR DP-LDPC CODES

The DP-LDPC code pairs proposed in [11] are simulated in Figure 3 for the JSCC system over on-body coding channel. The corresponding decoding thresholds are shown at the bottom of the curves. There is an error floor for each p where the code pair $\mathbf{B}_{0.06}^{s/c}$ derived in [11] cannot decode successfully in dash-line curves with "$\triangle$". To improve the error floors and decrease the code searching complexity, we redesign the DP-LDPC code pairs in the JSCC system with new methods.

A. CODE RATE DEFINITION OF DP-LDPC CODES IN THE JSCC SYSTEM

The source and channel code pairs are utilized by DP-LDPC codes in the JSCC system. A P-LDPC code of the source code is expressed with the protomatrix of dimensions $m_s \times n_s$, and the channel one is $m_c \times n_c$. Here, the code rate of the protomatrix is defined by the dimension.

The rate of the source protomatrix $\mathbf{B}_{sc}$ is defined by the protomatrix dimensions

$$R_1 = \frac{m_s}{n_s}, \quad (20)$$

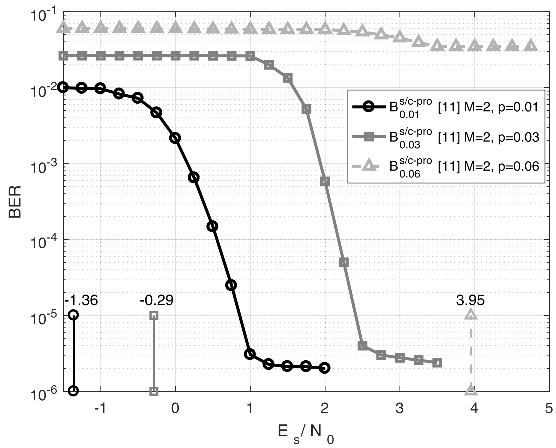

FIGURE 3. BER performances of DP-LDPC codes in [11] for different source statistics p via the 2-ary DCSK modulation over the on-body coding channel.

where m_s and n_s are the numbers of CNs and VNs of the source code protomatrix, respectively, and the rate of the channel $\mathbf{B}_{cc}$ is

$$R_2 = \frac{n_c - m_c}{n_c - n_p}, \quad (21)$$

where m_c and n_c are the numbers of CNs and VNs of the channel code protomatrix, respectively, $n_p = 1$ is a punctured VN in the column with the largest degree in the channel protomatrix.

The total code rate is

$$R = \frac{R_2}{R_1} = \frac{n_c - m_c}{n_c - 1} \times \frac{n_s}{m_s} := \frac{m_t}{n_t}. \quad (22)$$

The dimensions of the protomatrices of the total code rate are defined as $m_t = (n_c - m_c) \times n_s$ and $n_t = (n_c - 1) \times m_s$, respectively. Furthermore, the DP-LDPC codes utilized in the JSCC system should satisfy the relationship $n_c - m_s = m_c$ [14].

B. PDRS ALGORITHM FOR DP-LDPC CODES WITH CODE RATE BOUNDS

The optimal DP-LDPC code pair is searched by the DE Algorithm. Before searching the objective codes, the most appropriate dimensions of the DP-LDPC code pair for the proposed JSCC system should be firstly determined. In the JSCC system, the source code and the channel code are jointly decoded, where the redundant source is applied into the channel decoding for good BER performance. Therefore, the source-channel code rates need to be appropriately allocated for more source redundancy.

The source entropy and the channel capacity are the lower and upper bounds in communication system, respectively. The source code rate and the channel code rate are restrictively determined by the bound limitation.

(1) The minimum source code rate R_1 approaches the source entropy $H(p)$ according to the Shannon source coding theory [25]. In the JSCC system, the source code rate should be large to leave more source redundancy for channel

decoding to achieve low error floors, and satisfy:

$$\begin{aligned} \max \quad & \mathfrak{F}_1[\Delta D_s(R_1) = R_1 - H(p)] \\ s.t. \quad & 0 \le p \le 0.5, \\ & H(p) \le R_1, \\ & R_1 = \frac{m_s}{n_s}, \\ & 0 \le R_1 \le 1, \end{aligned} \tag{23}$$

where the function $\mathfrak{F}_1$ is defined by the differential value calculation ΔD_s.

(2) The maximum channel code rate R_2 is determined by the normalized channel capacity C according to the Shannon channel coding theory [25]. For a determinate channel capacity, the channel code rate is defined by the signal noise ratio (SNR) δ,

$$R_2 = \frac{C}{\log_2 M} = \frac{B \log_2(1+\delta)}{\log_2 M}, \tag{24}$$

where M represents the M-ary modulation order, and B is the bandwidth of the on-body channel. From Eq. (24), a higher channel code rate is achieved with a large δ value, which can be formalized as a differential value,

$$\begin{aligned} \max \quad & \mathfrak{F}_2[\Delta D_c(R_2) = 2^{\frac{R_2 \log_2 M}{B}} - 1] \\ s.t. \quad & B = 900MHz, \\ & R_2 = \frac{n_c - m_c}{n_c - 1}, \\ & 0 \le R_2 \le 1, \end{aligned} \tag{25}$$

where the function $\mathfrak{F}_2$ is defined by the deviation $\Delta D_c(\cdot)$.

The dimensions of the protomatrices are introduced to the code rate bound limitation in Eqs. (23) and (25). To determine the dimensions first, a restrictively searching algorithm with code rate bound is presented in Algorithm 1. The constraints of dimensions of the source-channel protomatrices are restrictively searching in lines 1 to 9 and lines 10 to 18, respectively. Then, line 21 is the constraint of the JSCC system that the utilized DP-LDPC code pair should follow [14]. Lines 22 and 23 ensure that the searched results by the source-channel code rates are positive and less than 1 according to Eq. (22).

From the proposed search algorithm 1, the dimensions of the DP-LDPC code pair are determined by the source statistic and the channel bandwidth. Thus, the size of the objective protomatrices with determined code rates can be obtained by the DE algorithm.

C. SIMPLIFIED JOINT PROTOMATRIX WITH NOVEL EDGE LINKING RELATIONSHIP

When the dimensions of the DP-LDPC code pairs are determined, the objective protomatrices are searched by the DE algorithm based on exhaustive entries search, which is time-consuming. The search process becomes more complex as the increase of the candidate number of searching code pairs with more entries. If the number of the induces of searching entries is decreased, the searching speed will be accelerated.

Algorithm 1 PDRS Algorithm for DP-LDPC Codes

Input:
n_t, m_t, p, B, M;
Output:
n_s, n_c, m_s, m_c;

1: ▷ the source code dimension-restrictive searching;
2: **for** each $m_s,\ n_s\ \in [1, 9]$ **do**
3: $n_s > m_s$;
4: **while** (max $\Delta D_s(R_1)$) **do**
5: **for all** n_s and m_s **do**
6: max $\mathfrak{F}_1 : \Delta D_s = \left[\frac{m_s}{n_s} - H(p)\right]$;
7: **end for**
8: **end while**
9: **end for**
10: ▷ the channel code dimension-restrictive searching;
11: **for** each $m_c,\ n_c\ \in [1, 9]$ **do**
12: $n_c > m_c$;
13: **while** (max $\Delta D_c(R_2)$) **do**
14: **for all** n_c and m_c **do**
15: max $\mathfrak{F}_2 : \Delta D_c = 2^{\frac{\log_2 M \times (n_c - m_c)}{B \times (n_c - 1)}} - 1$;
16: **end for**
17: **end while**
18: **end for**
19: ▷ the constraints of four searching dimensions;
20: **for all** output n_s, n_c, m_s and m_c **do**
21: $n_c - m_s = m_c$;
22: $m_t = (n_c - m_c) \times n_s, n_c > m_c$;
23: $n_t = (n_c - 1) \times m_s, n_s > m_s$;
24: **end for**

In [11], DP-LDPC codes are constructed to form a joint protomatrix with two linking matrices. The initial joint protomatrix is expressed as

$$\mathbf{B_J} = \begin{pmatrix} \mathbf{B}_{sc} & \mathbf{B}_{L1} \\ \mathbf{B}_{L2} & \mathbf{B}_{cc} \end{pmatrix}, \tag{26}$$

where $\mathbf{B}_{L2}$ and $\mathbf{B}_{L1}$ are linking matrices between the CNs (VNs) and VNs (CNs) connecting the source code with the channel code, respectively, and $\mathbf{B}_{sc}$ and $\mathbf{B}_{cc}$ are the protomatrices of the source code and the channel code, respectively.

To further accelerate the code search process, the joint protomatrix is reconstructed according to the new edge linking relationship in the JPEXIT algorithm as two simpler structures to decrease the number of induces of searching entries.

The initial JPEXIT algorithm [17] yields $I_{cc\to sc}(\jmath)$, which is the EMI between the LLR sent from $v_\jmath$ in $\mathbf{B}_{cc}$ to $c_\imath$ in $\mathbf{B}_{sc}$. Here, $I_{cc\to sc}(\jmath)$ is exchanged between the m_s CNs in the source code and the last m_s VNs in the channel code for one-to-one correspondence, that is, the last CN in the source code can only connect the last VN in the channel code. On the contrary, to obtain better BER performances, the joint protomatrix here is modified to be a one-to-n correspondence

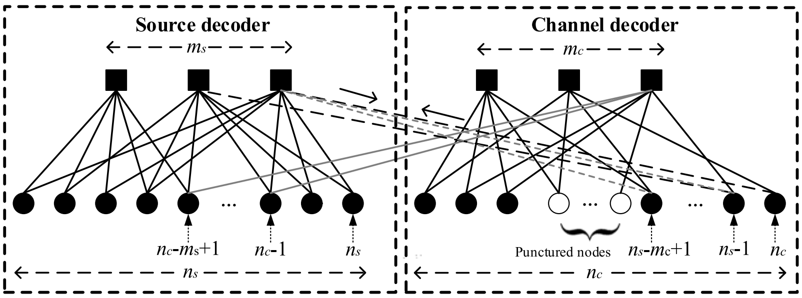

FIGURE 4. Block diagram of the joint source-channel decoding part of the modified edge linking relationship in the JPEXIT algorithm.

relationship of the last node in the source and channel codes. With a novel edge linking relationship, the joint protomatrix is simplified into two conditions as follows,

$$\mathbf{B_J} = \begin{pmatrix} \text{Bsc} & \mathbf{B}_{\ell 1} \\ & \mathbf{B}_{cc} \end{pmatrix} \tag{27}$$

or

$$\mathbf{B_J} = \begin{pmatrix} \mathbf{B}_{sc} & \text{Bcc} \\ \mathbf{B}_{\ell 2} & \end{pmatrix}. \tag{28}$$

The dimension of $\mathbf{B}_{sc}$ is $m_s \times n_s$ and the dimension of $\mathbf{B}_{cc}$ is $m_c \times n_c$, where m_s, n_s and m_c, n_c are the numbers of CNs and VNs in the DP-LDPC codes, respectively. If $m_s > m_c$, then the size of the linking matrix $\mathbf{B}_{\ell 1}$ is $(m_s - m_c) \times n_c$. If $m_s < m_c$, then the size of the linking matrix $\mathbf{B}_{\ell 2}$ is $(m_c - m_s) \times n_s$. If $m_s = m_c$, there are no $\mathbf{B}_{\ell 1}$ and $\mathbf{B}_{\ell 2}$.

With the increase of linking degrees in matrix $\mathbf{B}_{\ell 1}$ ($\mathbf{B}_{\ell 2}$), the last $m_s - m_c$ ($m_c - m_s$) CNs are more likely to be connected with multiple VNs, as is highlighted in Figure 4. In the figure, black squares and circles are the CNs and VNs, respectively, and hollow circles are the punctured VNs. $\mathbf{B}_{\ell 1}$ matrix is presented by the gray dash edges linking relationship, where the number of VNs satisfies $m_c \leq n_s - 1$. $\mathbf{B}_{\ell 2}$ matrix is presented by the gray solid edges linking relationship, where the number of VNs satisfies $m_s \leq n_c - 1$. The number of punctured VNs is n_p.

The dimensions of the objective code pairs are optimally obtained by the PDRS algorithm, and then searched by the DE algorithm. The PDRS algorithm is designed with universality, to be appropriate for different constructions, like Eq. (26). To simplify the DE searching cost, the constructions of Eqs. (27) and (28) are the main concern.

D. OPTIMAL DESIGN CRITERIA OF DECODING THRESHOLD FOR THE DP-LDPC CODE PAIR

The JPEXIT algorithm is introduced to provide a decoding threshold for searching the objective DP-LDPC codes. To well match the on-body channel characters, the channel LLR in JPEXIT is modified as follows.

- Initialization of the on-body channel variance for $j = 1, \ldots, n_c$ as

$$\sigma_{x,j}^2 = \mathcal{L}_{ch} \cdot L(1, j), \tag{29}$$

where $L(1, j)$ is the punctured jth column with the biggest VN-degree of the channel code, and $\mathcal{L}_{ch}$ is expressed in Eq. (17).

To this end, the simplified number of linking edges shown in Figure 4 in the proposed JPEXIT algorithm [11] is modified as follows.

- Variable nodes in $\mathbf{B}_{cc}$ are linking with last check node in $\mathbf{B}_{sc}$ for updating the mutual information as the $\mathbf{B}_{\ell 1}$ matrix. For $j = n_s - m_c + 1, \ldots, n_s - 1$ and $i = m_s - m_c + 1, \ldots, m_s$, if $b_{cc}^{i,j} \neq 0$, then

$$\begin{aligned} I_{sc \to cc}(j - (n_s - m_c)) \\ = 1 - J\left(\sqrt{\sum_i b_{sc}^{i,j}[J^{-1}(1 - I_{sc}^{Ac}(i, j))]^2}\right). \end{aligned} \tag{30}$$

where $b_{sc}^{i,j}$ is the degree of the source code $\mathbf{B}_{sc}$, representing the number of edges connecting the jth VN to the ith CN, $I_{sc}^{Ac}(i, j)$ is the PMI between the input LLR of the ith CN on each of the $b_{sc}^{i,j}$ linking edges and the associated jth VN.

- Variable nodes in $\mathbf{B}_{sc}$ are linking with last check node in $\mathbf{B}_{cc}$ for updating the mutual information as the $\mathbf{B}_{\ell 2}$ matrix. For $j = n_c - m_s + 1, \ldots, n_c - 1$ and $i = m_c - m_s + 1, \ldots, m_c$, if $b_{cc}^{i,j} \neq 0$, then

$$\begin{aligned} I_{cc \to sc}(j - (n_c - m_s)) \\ = J\left(\sqrt{\sum_i b_{cc}^{i,j}[J^{-1}(I_{cc}^{Av}(i, j))]^2 + \sigma_{x,j}^2}\right), \end{aligned} \tag{31}$$

where $b_{cc}^{i,j}$ is the degree of the channel code $\mathbf{B}_{cc}$, representing the number of edges connecting the jth VN to the ith CN, $I_{cc}^{Av}(i, j)$ is the PMI between the input LLR of the ith CN on each of the $b_{cc}^{i,j}$ linking edges and the associated jth VN, and $\sigma_{x,j}^2$ is the variance of the on-body coding channel in the jth VN.

The $J(\cdot)$ function is defined in [24] as the mutual information iterative convergence function between the input symbol X and the channel LLR $\mathcal{L}_{ch}$ given by

$$\begin{aligned} I(X; \mathcal{L}_{ch}) &= J(\sigma_x) \\ &= 1 - \int_{-\infty}^{\infty} \frac{e^{-(\xi - \sigma_x^2/2)/2\sigma_x^2}}{\sqrt{2\pi\sigma_x^2}} \cdot \log_2(1 + e^{-\xi}) d\xi, \end{aligned} \tag{32}$$

TABLE 2. The optimal dimensions of DP-LDPC codes allocated with total rate searched by the PDRS algorithm.

$R=\frac{m_t}{n_t}$	Source statistic	Code pair	m_s	n_s	ΔD_s	m_c	n_c	ΔD_c
2	$p=0.01$	$\mathbf{B}^{0.01}_{sc/cc-d}$	2	2	0.9192	3	5	3.8516e-04
		$\mathbf{B}^{s/c}_{0.01}$ [11]	2	8	0.1692	3	5	3.8516e-04
$\frac{8}{6}$	$p=0.03$	$\mathbf{B}^{0.03}_{sc/cc-d}$	4	8	0.3056	3	7	5.1357e-04
		$\mathbf{B}^{s/c}_{0.03}$ [11]	3	8	0.1806	4	7	3.8516e-04
1	$p=0.06$	$\mathbf{B}^{0.06}_{sc/cc-d}$	3	4	0.4226	2	5	5.7779e-04
		$\mathbf{B}^{s/c}_{0.06}$ [11]	3	8	0.0476	4	7	3.8516e-04

with

$$\lim_{\sigma_x\to 0} J(\sigma_x)=0,\ \lim_{\sigma_x\to\infty} J(\sigma_x)=1,\ \sigma_x>0. \tag{33}$$

The objective code pairs of the proposed JSCC system are searched to achieve a lower decoding threshold Γ_{TH} using the DE algorithm with fixed dimensions searched by Algorithm 1. The constrained optimization is

$$\begin{aligned} &\min\ [\mathfrak{F}_3(p)=\Gamma_{TH}]\\ &s.t.\ 0\le p\le 0.5,\\ &\quad I_{sc\to cc}>I^{-1}_{cc\to sc},\\ &\quad I_{sc\to cc}=I^{-1}_{cc\to sc}=1. \end{aligned} \tag{34}$$

Here, $I_{sc\to cc}(\jmath)$ is the EMI between the LLR sent by $c_\imath$ in $\mathbf{B}_{sc}$ to $v_\jmath$ in $\mathbf{B}_{cc}$, $I^{-1}_{cc\to sc}$ is the inverse of $I_{cc\to sc}$, and $\mathfrak{F}_3(\cdot)$ is defined by the redesigned JPEXIT algorithm. The first constraint is the feasible region of source statistics for the JSCC system. The last two constraints indicate that the joint source-channel decoding is decoded successfully.

IV. SIMULATION RESULTS AND DISCUSSION

A. THE DP-LDPC CODES SEARCHED WITH PDRS OPTIMAL DIMENSION

If a total rate R is given, the dimensions of the DP-LDPC codes are optimally achieved by Algorithm 1 for the JSCC system over on-body channel. The searched results are shown in Table 2. The differential values ΔD_s and ΔD_c are both larger than the ones in [11] according the objective functions of the code rate bound limitation in Eqs. (23) and (25). Here, the objective DP-LDPC codes are fixed with the dimensions by the PDRS algorithm and searched by the DE algorithm.

When $p=0.01$, the initialized searching joint protomatrix according to the Table 2, where $\mathbf{B}_{sc}=2\times 2$, $\mathbf{B}_{cc}=3\times 5$, $\mathbf{B}_{\ell 2}=1\times 2$ and $\mathbf{B}_{\ell 1}=0\times 0$, is expressed as

$$\mathbf{B}^{\mathbf{0.01}}_{\mathbf{J-ini}}=\begin{pmatrix} b^s_{11} & b^s_{12} & | & b^c_{11} & b^c_{12} & b^c_{13} & b^c_{14} & b^c_{15}\\ b^s_{21} & b^s_{22} & | & b^c_{21} & b^c_{22} & b^c_{23} & b^c_{24} & b^c_{25}\\ \hline 0 & 0 & | & b^c_{31} & b^c_{32} & b^c_{33} & b^c_{34} & b^c_{35} \end{pmatrix}, \tag{35}$$

where $b^s_{xy}, b^c_{xy}\in[0,1,2,3]$ are the degrees of linking edges between VNs (CNs) and CNs (VNs) in the source code and the channel code, respectively. $x,y\in\mathbb{N}^+$ and $\mathbb{N}^+$ is a set of positive integers. Since the number of linking VNs is $\jmath=n_c-m_s+1>m_s$, there is no degree in the matrix $\mathbf{B}_{\ell 2}$. The numbers of degree-1 and degree-2 VNs should satisfy the linear minimum distance growth principle [26], [27]. Then, the corresponding DE searching constraints with

$$\begin{cases} b^s_{1y}+b^s_{2y}\ge 3,\\ \Sigma_x b^c_{x1}=1,\\ \Sigma_x b^c_{x5}\ge 3,\\ \Sigma_x b^c_{x2}=\Sigma_x b^c_{x3}=\Sigma_x b^c_{x4}=2. \end{cases} \tag{36}$$

The searched code pairs are

$$\mathbf{B}^{0.01}_{sc-d}=\begin{pmatrix}2 & 3\\ 3 & 2\end{pmatrix}, \tag{37}$$

$$\mathbf{B}^{0.01}_{cc-d}=\begin{pmatrix}1 & 1 & 1 & 0 & 3\\ 0 & 1 & 1 & 1 & 2\\ 0 & 0 & 0 & 1 & 1\end{pmatrix}. \tag{38}$$

When $p=0.03$, the initialized searching joint protomatrix according to the Table 2, where $\mathbf{B}_{sc}=4\times 8$, $\mathbf{B}_{cc}=3\times 7$, $\mathbf{B}_{\ell 1}=1\times 7$ and $\mathbf{B}_{\ell 2}=0\times 0$, is expressed as (39), shown at the bottom of the page.

Since the VNs are linked from $\jmath=n_s-m_c+1=6$ to $\jmath=n_s-1=7$, there are two degree-1 VNs in the sixth and seventh columns of matrix $\mathbf{B}_{\ell 1}$, respectively. The corresponding DE searching constraints are

$$\begin{cases} b^s_{1y}+b^s_{2y}+b^s_{3y}+b^s_{4y}\ge 3,\\ \Sigma_x b^c_{x1}=\Sigma_x b^c_{x6}=1,\\ \Sigma_x b^c_{x7}\ge 3,\\ \Sigma_x b^c_{x2}=\Sigma_x b^c_{x3}=\Sigma_x b^c_{x4}=\Sigma_x b^c_{x5}=2. \end{cases} \tag{40}$$

$$\mathbf{B}^{\mathbf{0.03}}_{\mathbf{J-ini}}=\begin{pmatrix} b^s_{11} & b^s_{12} & b^s_{13} & b^s_{14} & b^s_{15} & b^s_{16} & b^s_{17} & b^s_{18} & | & 0 & 0 & 0 & 0 & 0 & 1 & 1\\ \hline b^s_{21} & b^s_{22} & b^s_{23} & b^s_{24} & b^s_{25} & b^s_{26} & b^s_{27} & b^s_{28} & | & b^c_{11} & b^c_{12} & b^c_{13} & b^c_{14} & b^c_{15} & b^c_{16} & b^c_{17}\\ b^s_{31} & b^s_{32} & b^s_{33} & b^s_{34} & b^s_{35} & b^s_{36} & b^s_{37} & b^s_{38} & | & b^c_{21} & b^c_{22} & b^c_{23} & b^c_{24} & b^c_{25} & b^c_{26} & b^c_{27}\\ b^s_{41} & b^s_{42} & b^s_{43} & b^s_{44} & b^s_{45} & b^s_{46} & b^s_{47} & b^s_{48} & | & b^c_{31} & b^c_{32} & b^c_{33} & b^c_{34} & b^c_{35} & b^c_{36} & b^c_{37} \end{pmatrix}. \tag{39}$$

TABLE 3. The number of indices of searching entries of the joint protomatrix.

Joint protomatrix	Number of indices of searching entries	Joint protomatrix	Number of indices of searching entries
$\mathbf{B_J^{0.01}}$	21	$\mathbf{B_J^{0.01}}$ [11]	65
$\mathbf{B_J^{0.03}}$	60	$\mathbf{B_J^{0.03}}$ [11]	105
$\mathbf{B_J^{0.06}}$	27	$\mathbf{B_J^{0.06}}$ [11]	105

The searched code pairs are

$$\mathbf{B}_{sc-d}^{0.03} = \begin{pmatrix} 1 & 2 & 1 & 1 & 3 & 2 & 1 & 0 \\ 1 & 1 & 2 & 1 & 2 & 3 & 3 & 1 \\ 2 & 1 & 0 & 2 & 2 & 1 & 2 & 1 \\ 0 & 0 & 2 & 3 & 0 & 1 & 3 & 1 \end{pmatrix}, \tag{41}$$

$$\mathbf{B}_{cc-d}^{0.03} = \begin{pmatrix} 1 & 1 & 0 & 1 & 1 & 1 & 3 \\ 0 & 1 & 1 & 1 & 1 & 0 & 2 \\ 0 & 0 & 1 & 0 & 0 & 0 & 3 \end{pmatrix}. \tag{42}$$

When $p = 0.06$, the initialized searching joint protomatrix according to the Table 2, where $\mathbf{B}_{sc} = 3 \times 4$, $\mathbf{B}_{cc} = 2 \times 5$, $\mathbf{B}_{\ell 1} = 1 \times 5$ and $\mathbf{B}_{\ell 2} = 0 \times 0$, is expressed as

$$\mathbf{B_{J-ini}^{0.06}} = \left(\begin{array}{cccc|ccccc} b^s_{11} & b^s_{12} & b^s_{13} & b^s_{14} & 0 & 0 & 1 & 0 & 0 \\ \cline{5-9} b^s_{21} & b^s_{22} & b^s_{23} & b^s_{24} & b^c_{11} & b^c_{12} & b^c_{13} & b^c_{14} & b^c_{15} \\ b^s_{31} & b^s_{32} & b^s_{33} & b^s_{34} & b^c_{21} & b^c_{22} & b^c_{23} & b^c_{24} & b^c_{25} \end{array}\right). \tag{43}$$

Since the VNs are linked from $\jmath = n_s - m_c + 1 = 3$ to $\jmath = n_s - 1 = 3$, there is one degree-1 VN in the third column of matrix $\mathbf{B}_{\ell 1}$. The corresponding DE searching constraints are

$$\begin{cases} b^s_{1y} + b^s_{2y} + b^s_{3y} \geq 3, \\ \Sigma_x b^c_{x1} = 1, \\ \Sigma_x b^c_{x5} \geq 3, \\ \Sigma_x b^c_{x2} = \Sigma_x b^c_{x3} = \Sigma_x b^c_{x4} = 2. \end{cases} \tag{44}$$

The searched code pairs are

$$\mathbf{B}_{sc-d}^{0.06} = \begin{pmatrix} 1 & 3 & 0 & 1 \\ 1 & 1 & 1 & 0 \\ 2 & 0 & 3 & 2 \end{pmatrix}, \tag{45}$$

$$\mathbf{B}_{cc-d}^{0.06} = \begin{pmatrix} 1 & 1 & 1 & 1 & 1 \\ 0 & 1 & 1 & 1 & 3 \end{pmatrix}. \tag{46}$$

The number of indices of searching entries is shown in Table 3, which is totally dropped in the simplified joint protomatrix compared with the one in [11]. Therefore, the searching cost of the DE algorithm is significantly decreased.

B. THE DP-LDPC CODES SEARCHED WITHOUT PDRS OPTIMAL DIMENSION

Referring to [11], the same dimensions of the DP-LDPC code pairs are straightly searched by the DE algorithm without the PDRS predesign for BER performance comparison.

When $p = 0.01$, the initialized searching joint protomatrix in [11], where $\mathbf{B}_{sc} = 2 \times 7$, $\mathbf{B}_{cc} = 3 \times 5$, $\mathbf{B}_{\ell 2} = 1 \times 7$ and $\mathbf{B}_{\ell 1} = 0 \times 0$, is expressed as (47), shown at the bottom of the page.

Since the VNs are linked from $\jmath = n_c - m_s + 1 = 4$ to $\jmath = n_c - 1 = 4$, there is one degree-1 VN in the fourth column of matrix $\mathbf{B}_{\ell 2}$. The corresponding DE searching constraints with

$$\begin{cases} b^s_{1y} + b^s_{2y} \geq 3, \\ \Sigma_x b^c_{x4} = 1, \\ \Sigma_x b^c_{x3} \geq 3, \\ \Sigma_x b^c_{x1} = \Sigma_x b^c_{x2} = \Sigma_x b^c_{x5} = 2. \end{cases} \tag{48}$$

The searched code pairs are

$$\mathbf{B}_{sc-nd}^{0.01} = \begin{pmatrix} 1 & 1 & 2 & 1 & 2 & 1 & 2 & 1 \\ 1 & 1 & 3 & 1 & 1 & 2 & 1 & 1 \end{pmatrix}, \tag{49}$$

$$\mathbf{B}_{cc-nd}^{0.01} = \begin{pmatrix} 0 & 0 & 3 & 1 & 0 \\ 1 & 1 & 2 & 0 & 1 \\ 1 & 1 & 1 & 0 & 1 \end{pmatrix}. \tag{50}$$

When $p = 0.03$, the initialized joint protomatrix in [11], where $\mathbf{B}_{sc} = 3 \times 8$, $\mathbf{B}_{cc} = 4 \times 7$, $\mathbf{B}_{\ell 2} = 1 \times 8$ and $\mathbf{B}_{\ell 1} = 0 \times 0$, is expressed as (51), shown at the bottom of the page.

Since the VNs are linked from $\jmath = n_c - m_s + 1 = 5$ to $\jmath = n_c - 1 = 6$, there are two degree-1 VNs in the fifth and sixth columns of $\mathbf{B}_{\ell 2}$, respectively. The corresponding DE searching constraints are

$$\begin{cases} b^s_{1y} + b^s_{2y} + b^s_{3y} \geq 3, \\ \Sigma_x b^c_{x1} = 1, \\ \Sigma_x b^c_{x5} = \Sigma_x b^c_{x6} = \Sigma_x b^c_{x7} \geq 3, \\ \Sigma_x b^c_{x2} = \Sigma_x b^c_{x3} = \Sigma_x b^c_{x4} = 2. \end{cases} \tag{52}$$

The searched code pairs are

$$\mathbf{B}_{sc-nd}^{0.03} = \begin{pmatrix} 1 & 3 & 1 & 1 & 2 & 1 & 1 & 1 \\ 1 & 2 & 1 & 2 & 1 & 1 & 1 & 1 \\ 1 & 1 & 2 & 1 & 1 & 2 & 1 & 1 \end{pmatrix}, \tag{53}$$

$$\mathbf{B_{J-ini}^{0.01}} = \left(\begin{array}{cccccccc|ccccc} b^s_{11} & b^s_{12} & b^s_{13} & b^s_{14} & b^s_{15} & b^s_{16} & b^s_{17} & b^s_{18} & b^c_{11} & b^c_{12} & b^c_{13} & b^c_{14} & b^c_{15} \\ b^s_{21} & b^s_{22} & b^s_{23} & b^s_{24} & b^s_{25} & b^s_{26} & b^s_{27} & b^s_{28} & b^c_{21} & b^c_{22} & b^c_{23} & b^c_{24} & b^c_{25} \\ \cline{1-8} 0 & 0 & 0 & 1 & 0 & 0 & 0 & 0 & b^c_{31} & b^c_{32} & b^c_{33} & b^c_{34} & b^c_{35} \end{array}\right). \tag{47}$$

$$\mathbf{B_{J-ini}^{0.03}} = \left(\begin{array}{cccccccc|ccccccc} b^s_{11} & b^s_{12} & b^s_{13} & b^s_{14} & b^s_{15} & b^s_{16} & b^s_{17} & b^s_{18} & b^c_{11} & b^c_{12} & b^c_{13} & b^c_{14} & b^c_{15} & b^c_{16} & b^c_{17} \\ b^s_{21} & b^s_{22} & b^s_{23} & b^s_{24} & b^s_{25} & b^s_{26} & b^s_{27} & b^s_{28} & b^c_{21} & b^c_{22} & b^c_{23} & b^c_{24} & b^c_{25} & b^c_{26} & b^c_{27} \\ b^s_{31} & b^s_{32} & b^s_{33} & b^s_{34} & b^s_{35} & b^s_{36} & b^s_{37} & b^s_{38} & b^c_{31} & b^c_{32} & b^c_{33} & b^c_{34} & b^c_{35} & b^c_{36} & b^c_{37} \\ \cline{1-8} 0 & 0 & 0 & 0 & 1 & 1 & 0 & 0 & b^c_{41} & b^c_{42} & b^c_{43} & b^c_{44} & b^c_{45} & b^c_{46} & b^c_{47} \end{array}\right). \tag{51}$$

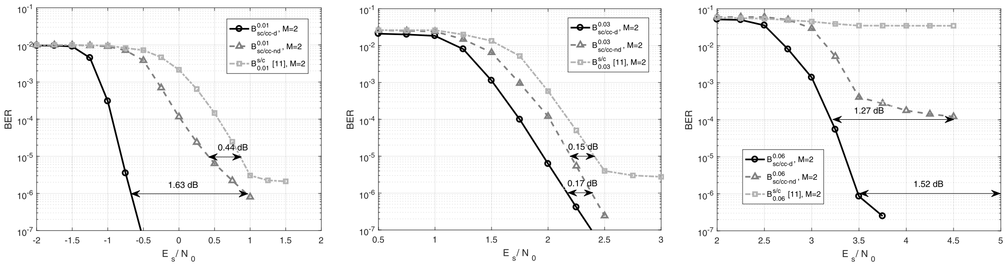

(a) $p = 0.01$ (b) $p = 0.03$ (c) $p = 0.06$

FIGURE 5. BER performances of DP-LDPC codes for different source statistics *p* via the 2-ary DCSK modulation over the on-body coding channel.

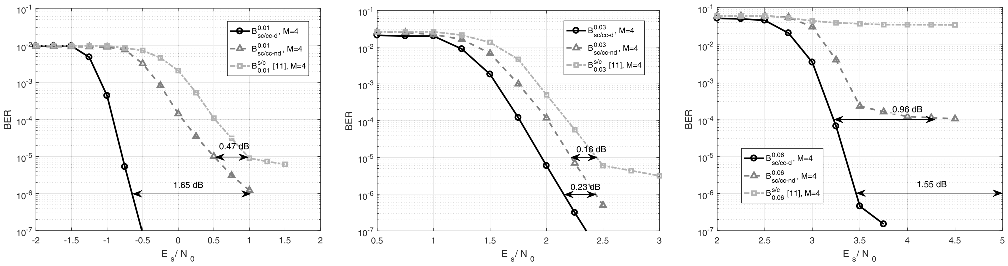

(a) $p = 0.01$ (b) $p = 0.03$ (c) $p = 0.06$

FIGURE 6. BER performances of DP-LDPC codes for different source statistics *p* via the 4-ary DCSK modulation over the on-body coding channel.

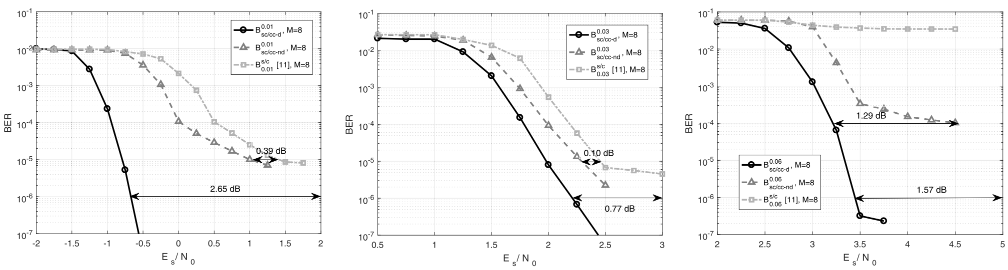

(a) $p = 0.01$ (b) $p = 0.03$ (c) $p = 0.06$

FIGURE 7. BER performances of DP-LDPC codes for different source statistics *p* via the 8-ary DCSK modulation over the on-body coding channel.

$$\mathbf{B}_{cc-nd}^{0.03} = \begin{pmatrix} 1 & 0 & 0 & 0 & 0 & 3 & 1 \\ 0 & 1 & 0 & 1 & 1 & 2 & 1 \\ 0 & 1 & 1 & 1 & 2 & 2 & 1 \\ 0 & 0 & 1 & 0 & 0 & 3 & 0 \end{pmatrix}, \tag{54}$$

When $p = 0.06$, the DP-LDPC code pair in [11] are faithfully decoding. The dimensions of the DE searching code pair are enlarged to achieve more source redundancy. Here, $\mathbf{B}_{sc} = 4 \times 8$, $\mathbf{B}_{cc} = 5 \times 9$, $\mathbf{B}_{\ell 2} = 1 \times 9$ and $\mathbf{B}_{\ell 1} = 0 \times 0$, the initialized joint protomatrix is expressed as (55), shown at the bottom of the page.

Since the VNs are linked from $\jmath = n_c - m_s + 1 = 6$ to $\jmath = n_c - 1 = 8$, there are three degree-1 VNs in the sixth, seventh and eighth columns of $\mathbf{B}_{\ell 2}$, respectively. The corresponding DE searching constraints are

$$\begin{cases} b_{1y}^s + b_{2y}^s + b_{3y}^s + b_{4y}^s \geq 3, \\ \Sigma_x b_{x1}^c = 1, \\ \Sigma_x b_{x6}^c = \Sigma_x b_{x7}^c = \Sigma_x b_{x8}^c = \Sigma_x b_{x9}^c \geq 3, \\ \Sigma_x b_{x2}^c = \Sigma_x b_{x3}^c = \Sigma_x b_{x4}^c = \Sigma_x b_{x5}^c = 2. \end{cases} \tag{56}$$

The searched code pairs are

$$\mathbf{B}_{sc-nd}^{0.06} = \begin{pmatrix} 1 & 3 & 1 & 1 & 1 & 1 & 1 & 2 \\ 1 & 2 & 1 & 2 & 1 & 0 & 1 & 1 \\ 1 & 1 & 1 & 1 & 1 & 1 & 3 & 1 \\ 1 & 0 & 2 & 1 & 2 & 1 & 1 & 1 \end{pmatrix}, \tag{57}$$

$$\mathbf{B}_{\mathbf{J-ini}}^{\mathbf{0.06}} = \left(\begin{array}{cccccccc|ccccccccc} b_{11}^s & b_{12}^s & b_{13}^s & b_{14}^s & b_{15}^s & b_{16}^s & b_{17}^s & b_{18}^s & b_{11}^c & b_{12}^c & b_{13}^c & b_{14}^c & b_{15}^c & b_{16}^c & b_{17}^c & b_{18}^c & b_{19}^c \\ b_{21}^s & b_{22}^s & b_{23}^s & b_{24}^s & b_{25}^s & b_{26}^s & b_{27}^s & b_{28}^s & b_{21}^c & b_{22}^c & b_{23}^c & b_{24}^c & b_{25}^c & b_{26}^c & b_{27}^c & b_{28}^c & b_{29}^c \\ b_{31}^s & b_{32}^s & b_{33}^s & b_{34}^s & b_{35}^s & b_{36}^s & b_{37}^s & b_{38}^s & b_{31}^c & b_{32}^c & b_{33}^c & b_{34}^c & b_{35}^c & b_{36}^c & b_{37}^c & b_{38}^c & b_{39}^c \\ b_{41}^s & b_{42}^s & b_{43}^s & b_{44}^s & b_{45}^s & b_{46}^s & b_{47}^s & b_{48}^s & b_{41}^c & b_{42}^c & b_{43}^c & b_{44}^c & b_{45}^c & b_{46}^c & b_{47}^c & b_{48}^c & b_{49}^c \\ \hline 0 & 0 & 0 & 0 & 0 & 1 & 1 & 1 & b_{51}^c & b_{52}^c & b_{53}^c & b_{54}^c & b_{55}^c & b_{56}^c & b_{57}^c & b_{58}^c & b_{59}^c \end{array}\right). \tag{55}$$

TABLE 4. Decoding threshold with different source statistics over log-normal on-body coding channel via searching code pairs.

Source statistics	Code pair	$\Gamma_{TH}^{M=2}$	$\Gamma_{TH}^{M=4}$	$\Gamma_{TH}^{M=8}$
$p = 0.01$	$\mathbf{B}_{sc/cc-d}^{0.01}$	-2.56 dB	-2.53 dB	-2.48 dB
	$\mathbf{B}_{sc/cc-nd}^{0.01}$	-1.65 dB	-1.61 dB	-1.58 dB
	$\mathbf{B}_{0.01}^{s/c}$ [11]	-1.36 dB	-1.41 dB	-1.43 dB
$p = 0.03$	$\mathbf{B}_{sc/cc-d}^{0.03}$	-0.73 dB	-0.69 dB	-0.65 dB
	$\mathbf{B}_{sc/cc-nd}^{0.03}$	-0.41 dB	-0.38 dB	-0.17 dB
	$\mathbf{B}_{0.03}^{s/c}$ [11]	-0.29 dB	-0.08 dB	0.23 dB
$p = 0.06$	$\mathbf{B}_{sc/cc-d}^{0.06}$	0.93 dB	0.99 dB	1.05 dB
	$\mathbf{B}_{sc/cc-nd}^{0.06}$	1.84 dB	1.86 dB	1.91 dB
	$\mathbf{B}_{0.06}^{s/c}$ [11]	3.95 dB	4.22 dB	4.31 dB

$$\mathbf{B}_{cc-nd}^{0.06} = \begin{pmatrix} 1 & 0 & 0 & 0 & 1 & 0 & 1 & 3 & 1 \\ 0 & 0 & 0 & 1 & 1 & 1 & 0 & 1 & 2 \\ 0 & 1 & 0 & 1 & 0 & 1 & 0 & 1 & 1 \\ 0 & 1 & 1 & 0 & 0 & 1 & 1 & 2 & 0 \\ 0 & 0 & 1 & 0 & 0 & 1 & 1 & 1 & 1 \end{pmatrix}. \quad (58)$$

C. THE COMPARISON OF DECODING THRESHOLD AND BER PERFORMANCE

Table 4 indicates that the decoding thresholds decrease when the source-channel code protomatrices predesigned by Algorithm 1 are utilized. In Figures 5-7, the BER performances and the system gains among different DP-LDPC codes are compared with three source statistics by M-ary DSCK modulation. In the fugures, the black solid line with circles simulates the decoding performance via the DP-LDPC codes predesigned by the PDRS algorithm, the gray dash line with triangles is the one without predesigning by the PDRS algorithm, and the light gray dash line with squares is the one proposed in [11].

Figures 5(a), 5(b) and 5(c) are the simulation results on the BER performances of the code pair $\mathbf{B}_{sc/cc-d}^{p}$ compared with the code pair $\mathbf{B}_{sc/cc-nd}^{p}$ and $\mathbf{B}_{p}^{s/c}$ [11] at $p = 0.01$, $p = 0.03$ and $p = 0.06$, respectively, where $M = 2$. For the DP-LDPC codes $\mathbf{B}_{p}^{s/c}$ derived in [11], there are error floors at different source statistics p. On the contrary, the waterfall regions of the predesigned code pair $\mathbf{B}_{sc/cc-d}^{p}$ in black appear at low E_s/N_0. By comparison of code pairs, one can see that the system gain is significantly increased at BER $= 10^{-6}$ with no error floor.

Simultaneously, the BER performances in Figures 6 and 7 show good waterfall regions and low power consumptions by the predesigned code pairs. Therefore, the predesign of the DP-LDPC code pairs by the PDRS algorithm is an effective way for the JSCC system to achieve higher reliability and lower power consumption over on-body channel.

V. CONCLUSION

We redesign the DP-LDPC codes in the JSCC system under different non-standard channels for the on-body coding channel. To match different channel characteristics well, some new optimal methods are proposed to redesign the DP-LDPC code pairs. The bound limitation of the code rate is introduced to restrictively search the most appropriate protomatrix dimension of the DP-LDPC codes, and the joint protomatrix is reconstructed into two simpler structures to further accelerate the code searching speed.

Referring to [3], the power consumption is SNR = 26 dB at BER $= 10^{-6}$ via the Bose-Chaudhuri-Hocquenghem (BCH 51,63) channel coding data over binary phase shift keying modulated channel in WBAN. Compared with the BER performance in the proposed JSCC system, it has lower power consumption because of the sparse source statistic. Most of the source information in WBAN follows the sparse distribution, therefore the JSCC system is a much more efficient paradigm for the WBAN data transmission on the physical layer.

To further construct a high reliability and low power consumption communication network, new efforts will be devoted to studying the intra-body channel model with the JSCC system to construct an integrated data transmission environment in WBAN in the future.

REFERENCES

[1] R. Cavallari, F. Martelli, R. Rosini, C. Buratti, and R. Verdone, "A survey on wireless body area networks: Technologies and design challenges," *IEEE Commun. Surveys Tuts.*, vol. 16, no. 3, pp. 1635–1657, 3rd Quart., 2014.

[2] J. Foerster, *Channel Modeling Subcommittee Report*, IEEE Standard P802.15-08-0780-09-0006, IEEE 802.15 Work Group Official Web Site, May 2003. [Online]. Available: http://grouper.ieee.org/groups/802/15/pub/2003/May03/

[3] H. Erdol, H. Y. Ozderya, C. Sisman, T. Kayikcioglu, and I. Kaya, "BER performance comparison of IEEE 802.15.6 and IEEE 802.15.4 on PHY layer," in *Proc. 39th Int. Conf. Telecommun. Signal Process. (TSP)*, Vienna, Austria, Jun. 2016, pp. 108–111.

[4] P. Chen, Z. Xie, Y. Fang, Z. Chen, S. Mumtaz, and J. J. P. C. Rodrigues, "Physical-layer network coding: An efficient technique for wireless communications," *IEEE Netw.*, vol. 34, no. 2, pp. 270–276, Mar./Apr. 2020.

[5] Y. Zhao, Y. Fang, and Z. Yang, "Interleaver design for small-coupling-length spatially coupled protograph LDPC-coded BICM systems over wireless fading channels," *IEEE Access*, vol. 8, pp. 33500–33510, 2020.

[6] J. Lee, K.-R. Lee, and H.-J. Yoo, "A 0.78 mW low-power 4.02 high-compression ratio less than 10^{-6} BER error-tolerant lossless image compression hardware for wireless capsule endoscopy system," in *Proc. IEEE Int. Symp. Circuits Syst. (ISCAS)*, Florence, Italy, May 2018, pp. 1–4.

[7] E. Reusens, W. Joseph, B. Latre, B. Braem, G. Vermeeren, E. Tanghe, L. Martens, I. Moerman, and C. Blondia, "Characterization of on-body communication channel and energy efficient topology design for wireless body area networks," *IEEE Trans. Inf. Technol. Biomed.*, vol. 13, no. 6, pp. 933–945, Nov. 2009.

[8] Q. Chen, L. Wang, P. Chen, and G. Chen, "Optimization of component elements in integrated coding systems for green communications: A survey," *IEEE Commun. Surveys Tuts.*, vol. 21, no. 3, pp. 2977–2999, 3rd Quart., 2019.

[9] G. Cai, Y. Fang, P. Chen, G. Han, G. Cai, and Y. Song, "Design of an MISO-SWIPT-Aided code-index modulated multi-carrier M-DCSK system for e-Health IoT," *IEEE J. Sel. Areas Commun.*, vol. 39, no. 2, pp. 311–324, Feb. 2021, doi: 10.1109/JSAC.2020.3020603.

[10] Y. Lyu, L. Wang, G. Cai, and G. Chen, "Iterative receiver for M-ary DCSK systems," *IEEE Trans. Commun.*, vol. 63, no. 11, pp. 3929–3936, Nov. 2015.

[11] Q. Chen and L. Wang, "Design and analysis of joint source channel coding schemes over non-standard coding channels," *IEEE Trans. Veh. Technol.*, vol. 69, no. 5, pp. 5369–5380, May 2020.

[12] G. Cai and Y. Song, "Closed-form BER expressions of M-ary DCSK systems over multipath Rayleigh fading channels," *IEEE Commun. Lett.*, vol. 24, no. 6, pp. 1192–1196, Jun. 2020.

[13] G. Cai, Y. Fang, J. Wen, S. Mumtaz, Y. Song, and V. Frascolla, "Multi-carrier M-ary DCSK system with code index modulation: An efficient solution for chaotic communications," *IEEE J. Sel. Topics Signal Process.*, vol. 13, no. 6, pp. 1375–1386, Oct. 2019.

[14] M. Fresia, F. Perez-Cruz, H. V. Poor, and S. Verdu, "Joint source and channel coding," *IEEE Signal Process. Mag.*, vol. 27, no. 6, pp. 104–113, Nov. 2010.

[15] L. Xu, L. Wang, S. Hong, and H. Wu, "New results on radiography image transmission with unequal error protection using protograph double LDPC codes," in *Proc. 8th Int. Symp. Med. Inf. Commun. Technol. (ISMICT)*, Firenze, Italy, Apr. 2014, pp. 1–4.

[16] J. He, Y. Li, G. Wu, S. Qian, Q. Xue, and T. Matsumoto, "Performance improvement of joint source-channel coding with unequal power allocation," *IEEE Wireless Commun. Lett.*, vol. 6, no. 5, pp. 582–585, Oct. 2017.

[17] H. Wu, L. Wang, S. Hong, and J. He, "Performance of joint source-channel coding based on protograph LDPC codes over Rayleigh fading channels," *IEEE Commun. Lett.*, vol. 18, no. 4, pp. 652–655, Apr. 2014.

[18] C. Chen, L. Wang, and F. C. M. Lau, "Joint optimization of protograph LDPC code pair for joint source and channel coding," *IEEE Trans. Commun.*, vol. 66, no. 8, pp. 3255–3267, Aug. 2018.

[19] H. V. B. Neto and W. Henkel, "Multi-edge optimization of low-density parity-check codes for joint source-channel coding," in *Proc. 9th Int. ITG Conf. Syst., Commun. Coding (SCC)*, München, Deutschland, 2013, pp. 1–6.

[20] S. Liu, L. Wang, J. Chen, and S. Hong, "Joint component design for the JSCC system based on DP-LDPC codes," *IEEE Trans. Commun.*, vol. 68, no. 9, pp. 5808–5818, Sep. 2020.

[21] Q. Chen, S. Hong, and Y. Chen, "Design of linking matrix in JSCC scheme based on double protograph LDPC codes," *IEEE Access*, vol. 7, pp. 92176–92183, 2019.

[22] Q. Chen, L. Wang, S. Hong, and Y. Chen, "Integrated design of JSCC scheme based on double protograph LDPC codes system," *IEEE Commun. Lett.*, vol. 23, no. 2, pp. 218–221, Feb. 2019.

[23] C. Abou-Rjeily and M. Bkassiny, "On the achievable diversity orders over non-severely faded lognormal channels," *IEEE Commun. Lett.*, vol. 14, no. 8, pp. 695–697, Aug. 2010.

[24] S. T. Brink, "Convergence behavior of iteratively decoded parallel concatenated codes," *IEEE Trans. Commun.*, vol. 49, no. 10, pp. 1727–1737, Nov. 2001.

[25] T. M. Cover and J. A. Thamos, *Elements of Information Theory*, 2nd ed. Hoboken, NJ, USA: Wiley, 2006.

[26] Q. Chen, L. Wang, Y. Lyu, and G. Chen, "Designing protograph-based LDPC codes for iterative receivers on M-ary DCSK systems," *IEEE Trans. Circuits Syst. II, Exp. Briefs*, vol. 65, no. 4, pp. 466–470, Apr. 2018.

[27] D. Divsalar, S. Dolinar, C. Jones, and K. Andrews, "Capacity-approaching protograph codes," *IEEE J. Sel. Areas Commun.*, vol. 27, no. 6, pp. 876–888, Aug. 2009.

[28] L. Chen, P. Chen, and Z. Lin, "Artificial intelligence in education: A review," *IEEE Access*, vol. 8, pp. 75264–75278, 2020.

[29] Y. Fang, P. Chen, G. Cai, F. C. M. Lau, S. C. Liew, and G. Han, "Outage-limit-approaching channel coding for future wireless communications: Root-protograph low-density parity-check codes," *IEEE Veh. Technol. Mag.*, vol. 14, no. 2, pp. 85–93, Jun. 2019.

DAN SONG received the B.Sc. degree in electronic information science and technology from Shangluo University, Shangluo, China, in 2016, and the M.Sc. degree in communication and information system from Northwest University, Xi'an, China, in 2019. She is currently pursuing the Ph.D. degree with the Department of Information and Communication Engineering, Xiamen University, Xiamen, China. Her research interests include joint source-channel coding, wireless body area networks, and quantum communication.

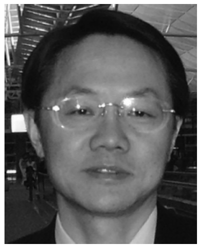

LIN WANG (Senior Member, IEEE) received the Ph.D. degree in electronics engineering from the University of Electronic Science and Technology of China, Chengdu, China, in 2001.

From 1984 to 1986, he was a Teaching Assistant with the Mathematics Department, Chongqing Normal University. From 1989 to 2002, he was Teaching Assistant, a Lecturer, and an Associate Professor of applied mathematics and communication engineering with the Chongqing University of Post and Telecommunication, Chongqing, China. From 1995 to 1996, he spent one year with the Mathematics Department, University of New England, Armidale, NSW, Australia. He spent three months as a Visiting Researcher with the Center for Chaos and Complexity Networks, City University of Hong Kong, in 2003. From 2012 to 2017, he was a Distinguished Professor with Xiamen University, China, where he has been a Full Professor with the School of Informatics, since 2003. He was a Senior Visiting Researcher with the Department of Electrical and Computer Engineering (ECE), University of California at Davis, Davis, CA, USA, in 2013. He has authored more than 200 journal and conference papers (including 63 IEEE journal articles). He holds 21 patents in physical layer in digital communications. His current research interests include source coding/channel coding, joint source and channel coding/decoding, chaos modulation and their applications to wired/wireless communications, and underwater acoustic communications.

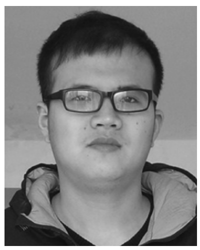

QIWANG CHEN received the B.Sc. degree in electronic science and technology from Huaqiao University, Xiamen, China, in 2012, and the Ph.D. degree in communication engineering from Xiamen University, Xiamen, in 2018. He was a Visiting Ph.D. student with the Faculty of Engineering, Monash University, Australia. He is currently a Lecturer with the School of Information Science and Engineering, Huaqiao University. His research interests include information theory and coding, joint source-channel coding, chaos communication, and the Internet of Things.

GUANRONG CHEN (Life Fellow, IEEE) received the M.Sc. degree in computer science from Sun Yat-sen University, Guangzhou, China, in 1981, and the Ph.D. degree in applied mathematics from Texas A&M University, College Station, TX, USA, in 1987. He was a tenured Full Professor with the University of Houston, Houston, TX. Since 2000, he has been a Chair Professor and the Founding Director of the Centre for Chaos and Complex Networks, City University of Hong Kong. He is a member of the Academy of Europe and a Fellow of The World Academy of Sciences. He received the State Natural Science Award of China, in 2008, 2012, and 2016, respectively. He was awarded the 2011 Euler Gold Medal, Russia, and conferred Honorary Doctorates by the Saint Petersburg State University, Russia, in 2011, and by the University of Le Havre, Normandy, France, in 2014. Since 2009, he has been a Highly Cited Researcher in Engineering according to Thomson Reuters.